

High-power femtosecond mid-infrared optical parametric oscillator at 7 μm based on CdSiP_2

S. Chaitanya Kumar,^{1,*} J. Krauth,² A. Steinmann,² K. T. Zawilski,³ P. G. Schunemann,³
H. Giessen,² and M. Ebrahim-Zadeh^{1,4}

¹ICFO-Institut de Ciències Fotoniques, Mediterranean Technology Park, 08860 Castelldefels, Barcelona, Spain

²4th Physics Institute and Research Center SCOPE, University of Stuttgart, Pfaffenwaldring 57, 70550 Stuttgart, Germany

³BAE Systems, Incorporated, MER15-1813, P.O. Box 868, Nashua, New Hampshire 03061-0868, USA

⁴Institució Catalana de Recerca i Estudis Avançats (ICREA), Passeig Lluís Companys 23, Barcelona 08010, Spain

*Corresponding author: chaitanya.suddapalli@icfo.es

Received January 22, 2015; revised February 23, 2015; accepted February 24, 2015;
posted February 25, 2015 (Doc. ID 233135); published March 24, 2015

We report a femtosecond optical parametric oscillator (OPO) for the mid-infrared (mid-IR), generating a record average power of 110 mW at 7 μm . The OPO, based on CdSiP_2 (CSP) as the nonlinear crystal, provides idler wavelength tuning across 6540–7186 nm with spectral bandwidths >400 nm at -10 dB level over the entire range, and a maximum bandwidth of 478 nm at 6.9 μm . To the best of our knowledge, this is the highest average power generated from a femtosecond OPO in the deep mid-IR. The OPO also provides near-IR signal wavelengths tunable across 1204–1212 nm with a usable power of 450 mW in 418-fs pulses at 1207 nm. The simultaneously measured signal and idler power exhibit a passive stability better than 1.6% rms and 3% rms, respectively. A mid-IR idler spectral stability with a standard deviation of the frequency fluctuations better than 40 MHz over 15 min, limited by the measurement resolution, is realized. Using the mid-IR idler from the CSP OPO, we perform Fourier-transform spectroscopy to detect liquid phase organic solvent, toluene (C_7H_8), in the molecular fingerprint region. © 2015 Optical Society of America

OCIS codes: (190.4360) Nonlinear optics, devices; (190.7110) Ultrafast nonlinear optics; (190.4400) Nonlinear optics, materials; (190.4970) Parametric oscillators and amplifiers.

<http://dx.doi.org/10.1364/OL.40.001398>

High-power femtosecond sources providing broadband pulses with wide spectral coverage in the mid-infrared (mid-IR) are of great interest for a variety of applications including spectroscopy, frequency comb generation, and sensitive detection of gas and liquid phase chemical species [1]. Synchronously pumped optical parametric oscillators (OPOs) are versatile and practical sources of such radiation. However, the development of femtosecond OPOs for the mid-IR using the well-established oxide-based nonlinear crystals such as periodically poled LiNbO_3 is practically limited to ~ 5 μm , imposed by the onset of material absorption. As such, access to femtosecond pulses beyond 5 μm has relied on difference-frequency-generation (DFG) [2] or tandem OPO pumping [3,4] using non-oxide-based nonlinear crystals such as GaSe and AgGaSe_2 , or direct pumping of OPOs beyond 2 μm in combination with orientation-patterned GaAs [5] to avoid two-photon material absorption. On the other hand, the advancement of mid-IR femtosecond OPOs beyond 5 μm using technologically mature pump lasers near 1 μm is highly desirable by circumventing the scarcity of long-wavelength laser sources, complexities associated with external tandem OPOs, and power limitations of single-pass DFG techniques. In this context, the recently developed nonlinear material, cadmium silicon phosphide, CdSiP_2 (CSP), offers unique linear and nonlinear optical properties [6]. Its large bandgap, wide transparency range, high optical quality, improved thermal and optical properties, together with a high effective nonlinear coefficient ($d_{\text{eff}} \sim 84$ pm/V) make it an attractive nonlinear material for mid-IR generation. Very importantly, CSP can also be pumped near 1 μm under noncritical phase-matching (NCPM) to generate mid-IR radiation in the 6–8 μm wavelength range. Earlier reports on

ultrafast frequency conversion sources based on CSP include optical parametric generators [7] and OPOs [8] in the high-energy picosecond as well as femtosecond time-scales [9]. However, achieving high average output powers in the mid-IR wavelength range has been challenging.

Here we report a high-power femtosecond OPO for the mid-IR based on CSP, generating as much as 110 mW of average idler power at wavelengths as long as 7 μm , and tunable across 6540–7186 nm. The OPO is synchronously pumped by a Yb:KGW solid-state laser operating at 1029 nm, and generates idler bandwidths >400 nm at -10 dB level across the entire tuning range. Signal tuning is also available over 1204–1212 nm with a usable power of 450 mW in 418-fs pulses at 1207 nm. To our knowledge, this is the highest average power generated from a femtosecond OPO at such deep mid-IR wavelengths as long as 7 μm using any nonlinear material and the longest wavelength generated from an OPO based on CSP.

The schematic of the experimental setup is shown in Fig. 1. The Yb:KGW solid-state laser oscillator provides up to 5 W of average power in transform-limited ~ 560 fs pulses at 43.1 MHz repetition rate. The laser operates at a central wavelength of 1029 nm with a FWHM bandwidth of 2.3 nm [2], and is maintained at maximum power to ensure stable performance. A combination of a half-wave-plate and a polarizing beam-splitter is used as an attenuator, while a second half-wave-plate provides the required polarization for phase-matching in the CSP crystal. The pump beam is then focused to a waist radius of $w_0 \sim 50$ μm in the nonlinear crystal using a lens (L_1) of focal length $f = 200$ mm. The CSP crystal is 1-mm-long with a 4 mm \times 5 mm aperture, cut at $\theta = 90^\circ$ ($\phi = 45^\circ$) for type-I ($e \rightarrow oo$) NCPM at room temperature. Using

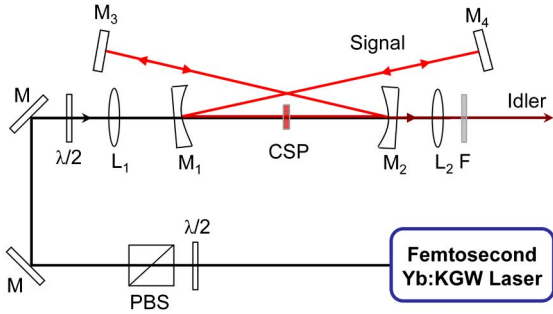


Fig. 1. Schematic of the experimental setup for the femtosecond OPO based on CSP. $\lambda/2$, half-wave plate; PBS, polarizing beam splitter; L, lens; M, mirrors; F, filter.

the relevant Sellmeier equations, the parametric gain bandwidth centered at 1029 nm, for a 1-mm-long CSP crystal, is estimated to be 10.6 nm [6], as shown in Fig. 2, relative to the pump spectrum. However, using the recently reported Sellmeier equations, a parametric gain bandwidth up to ~ 19 nm is estimated for the same CSP crystal [10]. As evident from Fig. 2, the entire pump spectrum lies well within the parametric gain bandwidth, implying the possibility of efficient nonlinear conversion. Also shown in the inset of Fig. 2 is the typical autocorrelation trace of the pump pulses, confirming a pulse duration of 557 fs, assuming sech^2 pulse shape. This pulse duration together with the 2.3-nm spectral bandwidth result in a transform-limited time-bandwidth product of $\Delta\tau\Delta\nu = 0.36$. The CSP crystal faces are both antireflection coated, providing high transmission for the pump ($T > 95\%$ at 1029 nm), signal ($T > 99\%$ over 1160–1240 nm), and idler ($T > 93\%$ over 6000–7500 nm). The OPO is designed in a four-mirror standing-wave cavity with two plano-concave mirrors, $M_{1,2}$ ($r = 150$ mm), and two plane mirrors, $M_{3,4}$. All mirrors are made of 3-mm-thick ZnSe substrate. The mirror coatings provide high transmission at the pump ($T > 82\%$ at 1029 nm) and idler ($T > 98\%$ over 6000–7500 nm), and high reflectivity for the signal ($R > 97\%$ over 1200–1230 nm), ensuring singly resonant signal oscillation. A CaF_2 lens, L_2 , is used to collect the idler, while a filter, F, separates the generated mid-IR idler from the residual pump. The total optical length of the cavity including the CSP crystal is

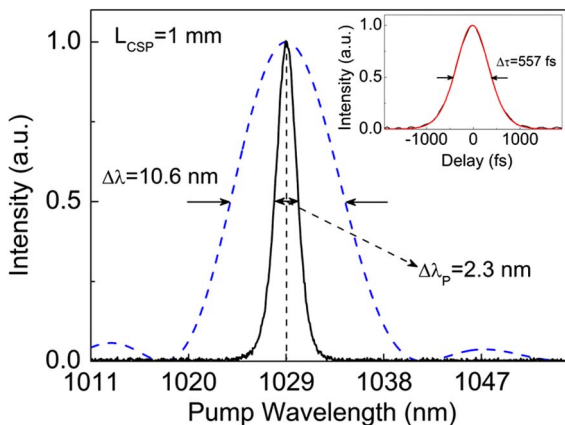


Fig. 2. Pump laser spectrum (solid line) relative to parametric gain bandwidth (dashed line) for a 1-mm-long CSP crystal. Inset: typical autocorrelation trace of the pump pulses.

1.74 m, corresponding to 86.2 MHz, ensuring synchronization at the second harmonic of the pump laser repetition rate.

As the pump wavelength of 1029 nm lies close to the short-wavelength transmission cut-off of the CSP crystal, significant losses due to linear as well as two-photon absorption are expected. Hence, before proceeding to characterize the OPO, we measured the residual losses at the pump wavelength. To perform these measurements, the pump beam was focused to a waist radius of $w_0 \sim 50$ μm in the CSP crystal, identical to that in the OPO, and we measured the transmitted power as a function of the input pump power. After correcting for the AR coating losses, the resulting transmission as a function of the input intensity was obtained for both *ordinary* (o) and *extraordinary* (e) polarizations. The results are shown in Fig. 3, where we observe a drop in the transmission of the CSP crystal with increasing pump intensity, confirming nonlinear behavior. The CSP transmission decreases from an initial value of 93% at a low intensity of ~ 57 MW/cm^2 down to 88% at an input intensity of ~ 2.4 GW/cm^2 for o -polarization. The corresponding drop for e -polarization is from 95% to 90%, implying better transmission for the required pump polarization for phase-matching. These measurements indicate better transmission characteristics than those previously reported [8,9], despite operating at very high intensities. Using a simple two-photon absorption model, we fitted the measured data for two-photon absorption coefficient (β), resulting in a value of $\beta_o = 0.27$ cm/GW for o -polarization and $\beta_e = 0.22$ cm/GW for e -polarization. These values of the two-photon absorption coefficient are lower than those measured using high-repetition-rate picosecond pulses at 1064 nm [8] and significantly lower than the value measured for the e -polarization using femtosecond pulses at 1053 nm [9]. This difference in the transmission characteristics could be attributed to the low repetition rate of the pump laser used in the present experiment. However, confirmation of the origin of this behavior requires further investigation. Using the obtained two-photon absorption coefficients, we have estimated the energy bandgap (E_g) of the material, resulting in a value of 2.35 eV for o -polarization and 2.36 eV for

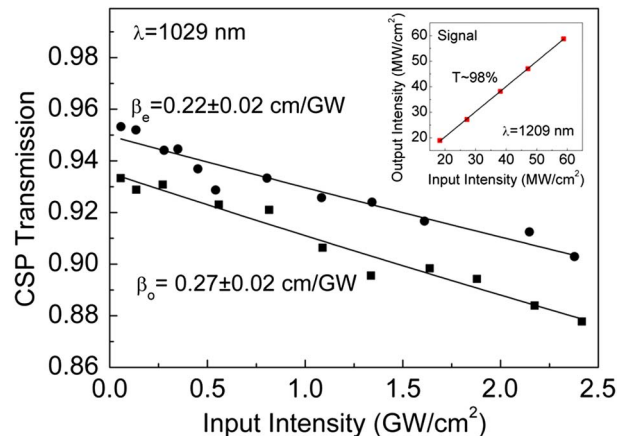


Fig. 3. CSP transmission as a function of pump intensity for e - and o -polarization at 1029 nm. Inset: CSP transmission measured at a signal wavelength of 1209 nm for o -polarization.

e-polarization, confirming the large bandgap of CSP [6]. We also performed similar measurements at the signal wavelength using the OPO output (*o*-polarization) up to a maximum intensity of ~ 60 MW/cm², as shown in the inset of Fig. 3, resulting in a transmission of $T \sim 98\%$ at an operating wavelength of 1209 nm.

Wavelength tuning of the CSP femtosecond OPO was achieved using cavity delay on either side of the perfectly synchronous cavity length. The generated idler spectra across the OPO tuning range are shown in Fig. 4(a). By varying the cavity delay, the idler central wavelength can be tuned over 240 nm, from 6760 to 7000 nm, in the mid-IR molecular fingerprint region. The corresponding idler spectral bandwidths at -10 dB are >400 nm over the entire tuning range extending from 6540 to 7186 nm, with a maximum of 478 nm at a central wavelength of $6.9 \mu\text{m}$. The modulation in the idler spectra could be attributed to the atmospheric absorption. The representative signal spectra across the OPO tuning range are also shown in Fig. 4(b), where the central signal wavelength can be tuned from 1204 to 1212 nm with -10 dB spectral bandwidths ranging from 17 to 12 nm over the full tuning range. The large parametric gain bandwidth of the CSP crystal suggests the potential for generating larger signal and idler bandwidths using a suitable broadband pump laser.

The power scaling results for the CSP femtosecond OPO are shown in Fig. 5. For a maximum available pump power of 3.7 W at the input to the nonlinear crystal, we were able to generate as much as 110 mW of idler output power at 7045 nm together with 225 mW signal power at 1205 nm from each plane end mirror, $M_{3,4}$, corresponding to a total usable signal output of 450 mW. The extraction of this high signal power is enabled by the partial transmission of $\sim 2.5\%$ in the signal wavelength range from each of the OPO cavity mirrors, amounting to a total signal loss of 10%, resulting in a usable signal output coupling of $\sim 5\%$ through the two plane end mirrors, $M_{3,4}$. The threshold of the OPO was ~ 700 mW, while a maximum pump depletion of $\sim 40\%$ was recorded. The slope efficiencies of the extracted signal and idler power are estimated to be 16% and 4%, respectively. Also shown in the inset of Fig. 5 is the depleted pump spectrum relative to the undepleted pump, centered at 1029 nm, clearly

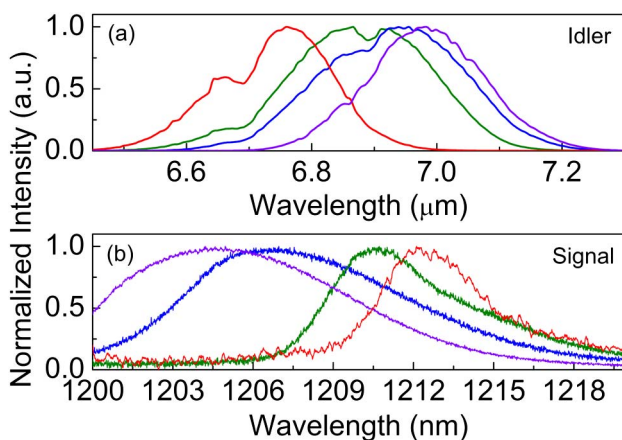


Fig. 4. (a) Idler and (b) signal spectra across the tuning range of the CSP femtosecond OPO obtained with cavity delay.

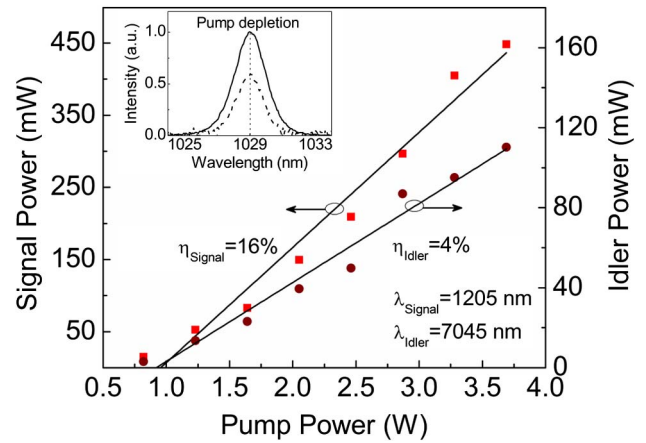


Fig. 5. Variation of the signal and idler average power from the CSP OPO as a function of pump power. Inset: pump spectrum before (solid line) and after (dashed line) the OPO, indicative of pump depletion.

confirming, efficient frequency conversion over the entire pump bandwidth and the large parametric gain bandwidth for the 1-mm-long CSP crystal.

We also investigated the long-term power stability of the idler and signal output from the OPO. Figure 6(a) shows the result measured at a central idler wavelength of 6977 nm. As can be seen, the idler is recorded to exhibit a passive power stability better than 3% rms over 1 h, while operating at an output power of ~ 100 mW. The simultaneously measured signal power at a central wavelength of 1207 nm exhibits a passive stability better than 1.6% rms over the same duration. We then performed the temporal and spectral measurements of the extracted signal pulses from the OPO, as shown in the inset of Fig. 6. The intensity autocorrelation trace of the signal pulses resulted in a sech^2 pulse duration of $\Delta\tau \sim 418$ fs in the absence of intracavity dispersion management. The corresponding signal spectrum was recorded to have a FWHM spectral width of 8.5 nm, centered at 1207 nm. These measurements correspond to a time-bandwidth product of $\Delta\tau\Delta\nu \sim 0.73$, which is twice the transform limit. The use of dispersion compensation in the OPO cavity could result in transform-limited output pulses.

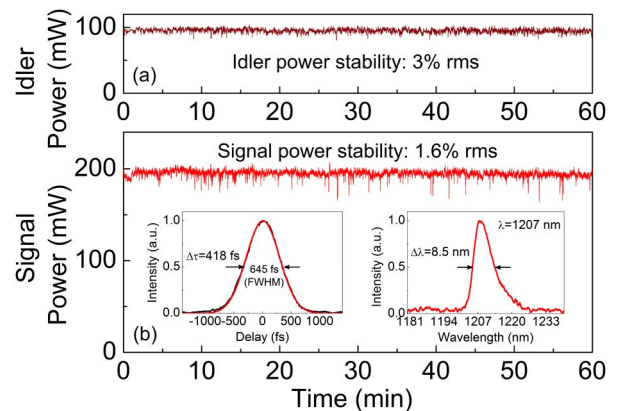


Fig. 6. Long-term average power stability of (a) idler and (b) signal output generated from the CSP femtosecond OPO. Inset: autocorrelation and spectral measurements of the signal pulses.

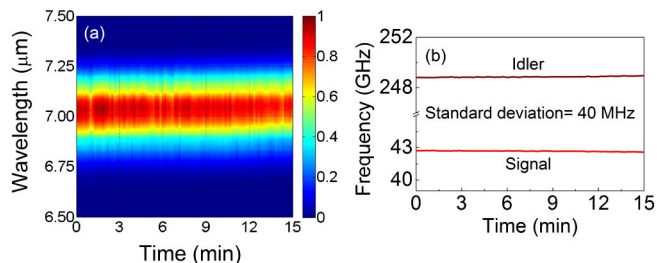


Fig. 7. (a) Mid-infrared idler passive spectral stability (color scale indicates normalized intensity) and (b) central wavelength stability of single and idler measured over 15 min.

Figure 7(a) shows the stability of the idler spectrum generated from the CSP OPO, recorded over a period of 15 min, resulting in a good frequency stability with a standard deviation better than 40 MHz, limited by the measurement resolution, at a central wavelength of $\sim 7 \mu\text{m}$ and 1206 nm for the signal and idler, respectively, as shown in Fig. 7(b).

Finally, we used the idler output from the CSP OPO to perform spectroscopic measurements of the liquid phase organic solvent, toluene (C_7H_8), in the mid-IR molecular fingerprint region. We applied a small drop of toluene sample on a CaF_2 substrate, and the spectrum was acquired in transmission geometry using a Fourier transform infrared (FTIR) spectrometer, while the idler from the OPO was used as the coherent mid-IR source. The measurement was averaged over 5 scans acquired at a speed of 0.5 cm/sec with a resolution of 2.3 nm (0.5 cm^{-1}). The normalized transmittance spectrum of toluene in the 6.5–7.2 μm ($1538\text{--}1389 \text{ cm}^{-1}$) wavelength range is shown in Fig. 8, in comparison with the reference spectrum from the NIST database, confirming good agreement.

In conclusion, we have demonstrated a femtosecond OPO for the mid-IR based on CSP, capable of providing a record average power of 110 mW at 7 μm . To our knowledge this is the highest deep mid-IR average power so far generated in the femtosecond time scale in any nonlinear material. The OPO idler central wavelength is tunable

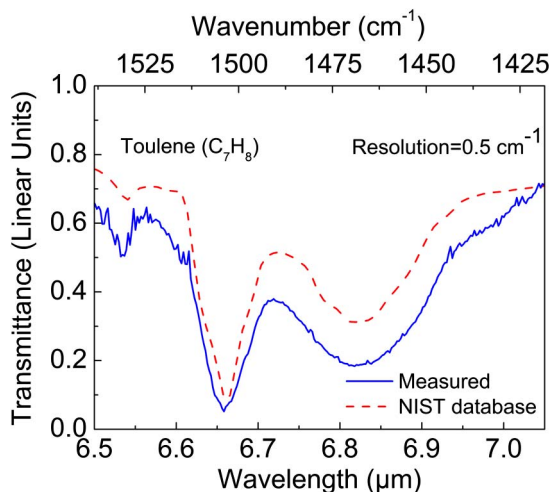


Fig. 8. Measured and reference transmittance spectrum of toluene on CaF_2 substrate acquired at spectral resolution of 2.3 nm (0.5 cm^{-1}) using the idler output from the CSP OPO and a FTIR spectrometer.

from 6760 to 7000 nm, with the -10 dB spectral coverage spanning across 6540–7186 nm. We have generated bandwidths $>400 \text{ nm}$ over the entire mid-IR tuning range, with a maximum bandwidth of 478 nm (-10 dB) at a central wavelength of 6.9 μm . The pump wavelength of 1029 nm is the shortest so far used to successfully pump a CSP OPO, while the mid-IR idler coverage represents the longest wavelengths generated with CSP to date. The OPO also provides signal tuning over 1204–1212 nm in 418-fs pulses at twice the transform limit without dispersion management. The simultaneous signal and idler passive power stability of the CSP OPO is better than 1.6% rms and 3% rms, respectively, and the mid-IR idler spectral stability with a standard deviation of the frequency fluctuations is better than 40 MHz over 15 min, limited by the measurement resolution. We have also demonstrated the utility of the OPO in FTIR spectroscopy of toluene using the mid-IR idler output. Further improvements in the output power can be achieved by optimizing the signal output coupling [11]. These results indicate that CSP is a highly promising material for practical development of deep mid-IR femtosecond OPOs, making the described system a viable and reliable source for many applications including ultrafast spectroscopy and frequency comb generation.

We acknowledge support from the Ministry of Economy and Competitiveness (MINECO), Spain (project OPTEX, TEC2012-37853), Generalitat de Catalunya (ACCIÓ, project VALTEC13-1-0003), European Office of Aerospace Research and Development (EOARD) (grant FA8655-12-1-2128), and the European Commission (project Mid-Tech). We would also like to thank ERC (Complexplas), COST (Nanospectroscopy), BW-Stiftung, DFG, BMBF, Zeiss-Stiftung, and AvH-Stiftung for their support.

References

1. A. Schliesser, N. Picqué, and T. W. Hänsch, *Nat. Photonics* **6**, 440 (2012).
2. J. Krauth, A. Steinmann, R. Hegenbarth, M. Conforti, and H. Giessen, *Opt. Express* **21**, 11516 (2013).
3. S. Marzenell, R. Beigang, and R. Wallenstein, *Appl. Phys. B* **69**, 423 (1999).
4. R. Hegenbarth, A. Steinmann, S. Mastel, S. Amarie, A. Huber, R. Hillenbrand, S. Sarkisov, and H. Giessen, *J. Opt.* **16**, 094003 (2014).
5. N. Leindecker, A. Marandi, R. L. Byer, K. L. Vodopyanov, J. Jiang, I. Hartl, M. Fermann, and P. G. Schunemann, *Opt. Express* **20**, 7046 (2012).
6. K. T. Zawilski, P. G. Schunemann, T. M. Pollak, D. E. Zelmon, N. C. Fernelius, and F. K. Hopkins, *J. Cryst. Growth* **312**, 1127 (2010).
7. S. Chaitanya Kumar, M. Jelínek, M. Baudisch, K. T. Zawilski, P. G. Schunemann, V. Kubeček, J. Biegert, and M. Ebrahim-Zadeh, *Opt. Express* **20**, 15703 (2012).
8. S. Chaitanya Kumar, A. Agnesi, P. Dalocchio, F. Pirzio, G. Reali, K. T. Zawilski, P. G. Schunemann, and M. Ebrahim-Zadeh, *Opt. Lett.* **36**, 3236 (2011).
9. Z. Zhang, D. T. Reid, S. Chaitanya Kumar, M. Ebrahim-Zadeh, P. G. Schunemann, K. T. Zawilski, and C. R. Howle, *Opt. Lett.* **38**, 5110 (2013).
10. V. Kemlin, P. Brand, B. Boulanger, P. Segonds, P. G. Schunemann, K. T. Zawilski, B. Ménaert, and J. Debray, *Opt. Lett.* **36**, 1800 (2011).
11. S. Chaitanya Kumar, A. Esteban-Martin, and M. Ebrahim-Zadeh, *Opt. Lett.* **36**, 1068 (2011).